BRAIN
ORIGINAL ARTICLE

Imaging meningeal inflammation in CNS autoimmunity identifies a therapeutic role for BTK inhibition

Pavan Bhargava,[1] Sol Kim,[1] Arthur A. Reyes,[1] Roland Grenningloh,[2] Ursula Boschert,[3] Martina Absinta,[1] Carlos Pardo,[1] Peter Van Zijl,[4] Jiangyang Zhang[5] and Peter A. Calabresi[1]

Leptomeningeal inflammation in multiple sclerosis is associated with worse clinical outcomes and greater cortical pathology. Despite progress in identifying this process in multiple sclerosis patients using post-contrast fluid-attenuated inversion recovery imaging, early trials attempting to target meningeal inflammation have been unsuccessful. There is a lack of appropriate model systems to screen potential therapeutic agents targeting meningeal inflammation. We utilized ultra-high field (11.7 T) MRI to perform post-contrast imaging in SJL/J mice with experimental autoimmune encephalomyelitis induced via immunization with proteolipid protein peptide ($PLP_{139–151}$) and complete Freund's adjuvant. Imaging was performed in both a cross-sectional and longitudinal fashion at time points ranging from 2 to 14 weeks post-immunization. Following imaging, we euthanized animals and collected tissue for pathological evaluation, which revealed dense cellular infiltrates corresponding to areas of contrast enhancement involving the leptomeninges. These areas of meningeal inflammation contained B cells (B220+), T cells (CD3+) and myeloid cells (Mac2+). We also noted features consistent with tertiary lymphoid tissue within these areas, namely the presence of peripheral node addressin-positive structures, C-X-C motif chemokine ligand-13 (CXCL13)-producing cells and FDC-M1+ follicular dendritic cells. In the cortex adjacent to areas of meningeal inflammation we identified astrocytosis, microgliosis, demyelination and evidence of axonal stress/damage. Since areas of meningeal contrast enhancement persisted over several weeks in longitudinal experiments, we utilized this model to test the effects of a therapeutic intervention on established meningeal inflammation. We randomized mice with evidence of meningeal contrast enhancement on MRI scans performed at 6 weeks post-immunization, to treatment with either vehicle or evobrutinib [a Bruton tyrosine kinase (BTK) inhibitor] for a period of 4 weeks. These mice underwent serial imaging; we examined the effect of treatment on the areas of meningeal contrast enhancement and noted a significant reduction in the evobrutinib group compared to vehicle (30% reduction versus 5% increase; $P = 0.003$). We used ultra-high field MRI to identify areas of meningeal inflammation and to track them over time in SJL/J mice with experimental autoimmune encephalomyelitis, and then used this model to identify BTK inhibition as a novel therapeutic approach to target meningeal inflammation. The results of this study provide support for future studies in multiple sclerosis patients with imaging evidence of meningeal inflammation.

1 Department of Neurology, Johns Hopkins University School of Medicine, Baltimore, MD, USA
2 EMD Serono Research and Development Institute, Inc., Billerica, MA, USA
3 Merck Serono SA, Eysin, Switzerland
4 F.M. Kirby Research Center for Functional Brain Imaging, Kennedy Krieger Institute, Baltimore, MD, USA
5 Department of Radiology, New York University, New York, NY, USA

Received July 8, 2020. Revised November 17, 2020. Accepted December 3, 2020. Advance access publication March 16, 2021

Correspondence to: Pavan Bhargava, MD
Department of Neurology, Johns Hopkins University School of Medicine
600 N Wolfe St, Pathology 627, Baltimore MD 21287, USA
E-mail: pbharga2@jhmi.edu

Keywords: EAE; leptomeningeal inflammation; BTK inhibition; B cell; astrocyte
Abbreviation: (rr)-EAE = (relapsing-remitting) experimental autoimmune encephalomyelitis

Introduction

Multiple sclerosis is a demyelinating disorder of the CNS that has both inflammatory and demyelinating components.[1] Leptomeningeal inflammation was first noted in patients with secondary progressive multiple sclerosis in 2004[2] and has subsequently been described in primary progressive multiple sclerosis and relapsing-remitting multiple sclerosis.[3,4] Meningeal inflammation may be organized as ectopic lymphoid follicles consisting of B cells, follicular-helper T cells and follicular dendritic cells, or may be unorganized consisting of lymphocytic and monocytic populations.[5,6] The presence of meningeal inflammation is linked to greater cortical demyelination and a more severe disease course, suggesting a role for meningeal inflammation in multiple sclerosis disease progression.[6,7] In individuals with multiple sclerosis, contrast-enhanced FLAIR imaging appears to detect areas of leptomeningeal contrast enhancement that correspond to areas of meningeal inflammation on autopsy.[5] More recent studies with 7 T MRI appear to demonstrate enhanced ability to detect this process in multiple sclerosis patients.[8,9] There is still controversy regarding the best approach to identify this phenomenon in patients and its relationship to cortical damage; however, all studies have shown a consistent relationship between cortical thinning and the presence of leptomeningeal enhancement.[5,8–14] Trials have been conducted to target meningeal inflammation,[15–18] but these attempts are hampered by the lack of appropriate models to screen potential therapies, especially those that could impact established meningeal inflammation.

Meningeal inflammation has been noted in animal models of multiple sclerosis, including the relapsing-remitting model of experimental autoimmune encephalomyelitis (rr-EAE) in SJL/J mice.[19–21] While meningeal inflammation is apparent in EAE prior to the onset of inflammation in the brain parenchyma, the cellular composition and contributors at this stage differ from those seen in multiple sclerosis meningeal tissue.[22,23] In EAE models with chronic expression of the B cell chemokine CXCL13 and BAFF (B-cell activating factor) in the CNS, evidence of meningeal inflammation with an abundance of B cells and evidence of tertiary lymphoid organ formation has been described.[2] In the rr-EAE model, the occurrence of leptomeningeal inflammation is variable and the composition of meningeal infiltrates appears to evolve over time—from predominantly T-cell to a T- and B-cell infiltrate—but has not been systematically studied.[20] There is also evidence for increased demyelination and axonal damage in areas of the spinal cord or cortex adjacent to areas of leptomeningeal inflammation in EAE similar to that seen in multiple sclerosis.[20,21] Thus, the leptomeningeal inflammation noted in rr-EAE mice appears to recapitulate several features seen in multiple sclerosis. However, since leptomeningeal inflammation is not uniform between mice, studying the effect of therapies on this phenomenon is challenging. Identification of meningeal inflammation on imaging and tracking its evolution over time provides an outcome that could be used to study the effect of interventions targeting meningeal inflammation. In this study we first describe the application of high-field contrast-enhanced MRI to identify and track meningeal inflammation in the rr-EAE model in SJL/J mice, providing a novel approach to screen therapies that could target this pathophysiological process.

A rational target potentially involved in leptomeningeal inflammation is Bruton tyrosine kinase (BTK), which transmits signals through a variety of receptors leading to B-cell and myeloid-cell activation and pro-inflammatory polarization.[24,25] From the various BTK inhibitors developed for clinical use, evobrutinib was the first to show clinical efficacy in EAE and in a relapsing-remitting multiple sclerosis phase 2 clinical trial.[26] Here, we use this model to examine the therapeutic effects of evobrutinib on meningeal inflammation, and provide evidence for potential utility of this class of medications in targeting this pathological process in patients with multiple sclerosis.

Materials and methods

Animals

SJL/J mice were purchased from Jackson Laboratories for all experiments. All mice were maintained in a federally approved animal facility at Johns Hopkins University in accordance with the Institutional Animal Care and Use Committee. Female mice aged 7–8 weeks were used in all experiments and were housed in the animal facility for 1 week prior to the start of experiments.

Induction of relapsing-remitting EAE

Female SJL/J mice were immunized subcutaneously at two sites over the lateral abdomen with 100 μg $PLP_{139-151}$ peptide with complete Freund's adjuvant containing 4 μg/ml *Mycobacterium tuberculosis* H37RA (Difco Laboratories). Mice were weighed and scored serially to document disease course. Scoring was performed using the following scale: 0, normal; 1, limp tail; 2, hind limb weakness; 3, hind limb paralysis; 4, forelimb weakness; and 5, death.

Imaging of meningeal disease

At the time points noted above, a horizontal 11.7 T scanner (Bruker BioSpin) with a triple-axis gradient system (maximum gradient strength = 740 mT/m), 72 mm volume transmit coil and 4-channel receive-only phased array coil was used to image the mouse forebrain. During imaging, mice were anaesthetized with isoflurane together with mixed air and oxygen (3:1 ratio) and respiration was monitored via a pressure sensor and maintained at 60 breaths/min. Before imaging, 0.1 ml diluted Magnevist® (gadopentetate dimeglumine, Bayer HealthCare LLC, 1:10 with PBS) was injected intraperitoneally and T_2-weighted images were acquired using a rapid acquisition with refocused echoes (RARE) sequence with the parameters: echo time/repetition time = 30/5000 ms; echo train length = 8, field of view = 15 mm × 15 mm, 30 axial slices with a slice thickness of 0.5 mm to cover the entire brain, matrix size = 192 × 192, and a signal average of 4. T_1-weighted images were acquired using a spin echo sequence with the same parameters as

the T_2-weighted images except echo time/repetition time = 9/300 ms, matrix size = 128 × 128, and only 15 axial slices were acquired to cover the forebrain region. FLAIR images were acquired using the RARE sequence with an inversion pulse. The imaging parameters were: echo time/repetition time = 20/3000 ms, steady-state inversion time = 1000 ms after a sech adiabatic inversion pulse, 15 axial slices with slice thickness of 0.5 mm, and the same matrix size and imaging geometry as the T_1-weighted images. 3D thick-slab MP-RAGE images of the forebrain were acquired in initial experiments with the following parameters: echo time/repetition time= 4/15 ms, four segments with a repetition time of 4000 ms, inversion time = 1000 ms with a sech adiabatic inversion pulse, four signal averages, field of view = 15 mm × 15 mm × 10 mm, and matrix size = 128 × 128 × 20. MP-RAGE images were not acquired in later experiments to shorten total imaging time required for sick animals.

Scans were then analysed to identify areas of meningeal contrast enhancement by at least two independent examiners (P.B., J.Z., S.K., M.A.). We utilized a semi-quantitative scheme to quantify the extent of meningeal contrast enhancement: we counted the number of areas of meningeal contrast enhancement on each individual MRI slice and used the cumulative number to represent the amount of meningeal contrast enhancement. All quantifications were performed by at least two independent examiners and their scores were averaged.

Histological identification of meningeal disease

Following the final imaging time point, mice were deeply anaesthetized with sodium pentobarbital (100 mg/kg) followed by intracardiac perfusion with 4% paraformaldehyde. The skull was separated, stripped of all soft tissue and placed in 14% EDTA at pH 7.6 for decalcification. Skulls were weighed daily to determine the time point of maximal decalcification. The decalcified skulls were transferred to 30% sucrose for 48 h and embedded in O.C.T. before snap-freezing. Tissues were cryosectioned at 10 μm thickness onto glass slides (SuperFrost Plus™, Fisher) to capture the appropriate brain and meningeal areas corresponding to meningeal enhancing lesions noted on MRI. Haematoxylin and eosin staining (Empire Genomics) was performed to verify that the appropriate areas had been captured during this process.

Immunohistochemistry to characterize meningeal disease

Blocking and permeabilization of sections was performed in PBS containing 5% normal goat serum (NGS) and 0.4% Triton™ X-100 for 1 h at room temperature followed by incubation overnight at 4°C in PBS containing 3% NGS, 0.1% Triton™ X-100, and primary antibodies. The optional antigen retrieval was performed with heated citrate buffer (pH 6) for 5–8 min before blocking. The slides were then washed and incubated with appropriate secondary antibodies conjugated to Alexa™ fluorophores (1:1000, Invitrogen), 3% NGS and 0.1% Triton™ X-100 for 1 h at room temperature. The slides were mounted using anti-fade reagent with DAPI (ProLong™ Gold Anti-fade Mountant, Gibco) and examined under a fluorescent microscope. The antibodies tested included APP, B220, CD3, CXCL13, FDC-M1, fibrinogen, GFAP, IBA-1, INOS, Mac2, SMI-32, and peripheral node addressin (PNAd) (see list of antibodies in Supplementary Table 1). For myelin staining, NovaUltra™ Luxol Fast Blue (IHC-WORLD) was used in accordance with the manufacturer's protocol.

Imaging was performed using an Olympus BX41, ZEISS Axio Cell Observer or ZEISS LSM 800 microscope with appropriate exposure and magnification. Each slide was imaged with one to two sections from each group (EAE versus naïve) and each panel was processed with ZEN lite (ZEISS) and National Institutes of Health ImageJ software (NIH, https://imagej.nih.gov/ij/).

Effect of evobrutinib treatment on leptomeningeal inflammation

Evobrutinib was obtained from EMD Serono and mice were treated with either vehicle solution (20% kleptose in 100 mM sodium citrate buffer, pH 3) or evobrutinib dissolved in vehicle solution by daily oral gavage (10 mg/kg) between Weeks 6 and 10 post-immunization. Each group (vehicle versus treatment) underwent contrast-enhanced MRI at Week 6, 8 and 10 and brain tissues were collected for histopathology at the final imaging time point. Meningeal contrast enhancement was quantified by raters blinded to treatment assignment at each imaging time point to assess the effect of interventions on meningeal inflammation.

Statistical analysis

Comparisons of pathological outcomes between groups were performed using a Mann-Whitney U-test. To compare the effects of vehicle versus evobrutinib on meningeal contrast enhancement in mice with EAE, a mixed effects model was used since we had repeated measures in each group. All analyses were performed using GraphPad Prism Version 8.3.0. The threshold for statistical significance was set at $P < 0.05$ for all tests.

Data availability

The data supporting the findings of this study are available within the article and its Supplementary material.

Results

MRI identifies areas of leptomeningeal contrast enhancement in SJL/J mice with EAE

To determine whether MRI can reveal meningeal inflammation in EAE, we immunized female SJL/J mice as described in the 'Materials and methods' section. The typical disease course in these mice is shown in Fig. 1A. We chose the SJL/J rr-EAE model for our experiments because previous studies have reported the development of meningeal inflammation with features of tertiary lymphoid tissue in this model.[19,20] In our initial cross-sectional experiments, we performed contrast-enhanced MRI scans at 6 weeks post-immunization. At this time point, the majority of mice had one or more contrast-enhancing lesions within the subarachnoid space (Fig. 1B). Some of these areas of contrast enhancement were noted on both T_1-weighted as well as FLAIR sequences. However, in common with human studies demonstrating the superiority of post-contrast FLAIR imaging for detecting leptomeningeal pathology,[5,27] FLAIR imaging also revealed more/larger areas of leptomeningeal contrast enhancement in our mice (Supplementary Fig. 1). Based on these findings, we therefore subsequently utilized FLAIR MRI to detect and monitor leptomeningeal contrast enhancement. Leptomeningeal contrast enhancement was detected both over the surface of the cerebral cortex and in the hippocampal fissure (Fig. 1B), but was not seen in control animals (Fig. 1C).

Additional experiments were performed at early (2 weeks post-immunization), middle (4–6 weeks post-immunization) and late (⩾8 weeks post-immunization) time points. An increase in the number and size of leptomeningeal contrast-enhancing lesions was seen at later time points (Fig. 1D).

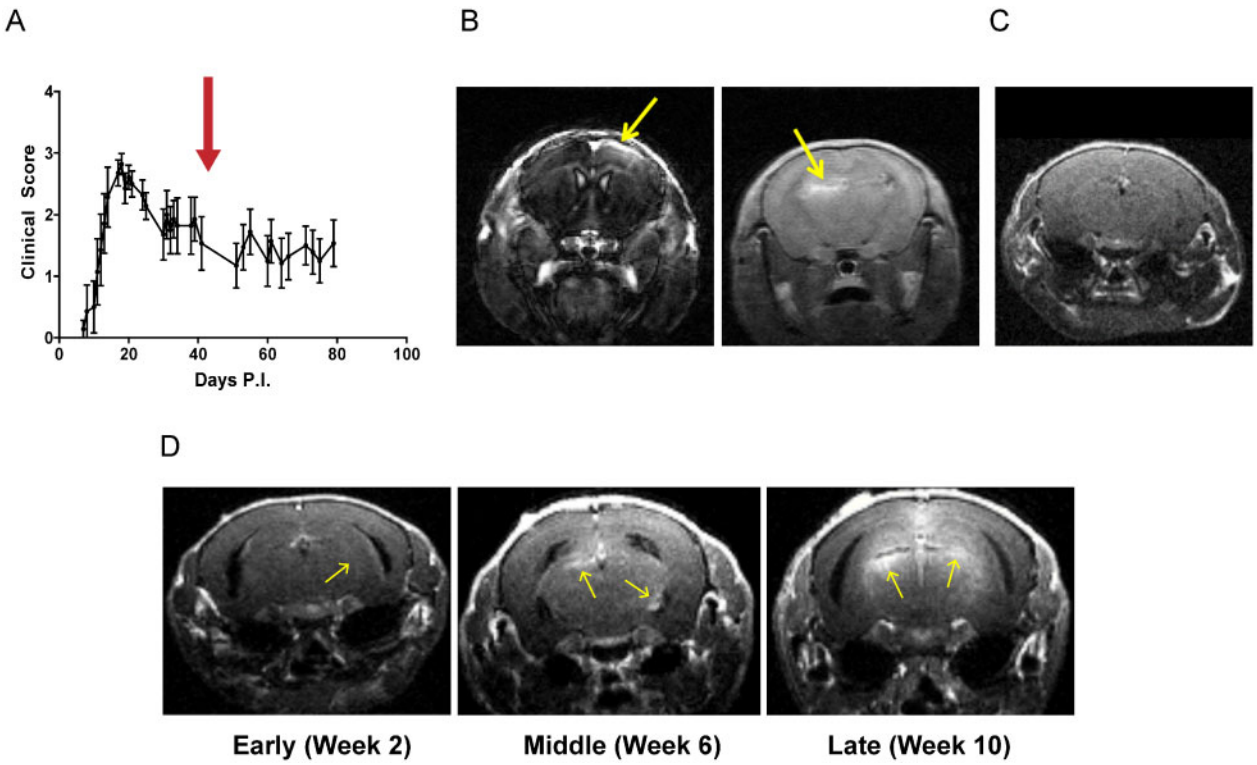

Figure 1 Ultra-high field MRI detects meningeal contrast enhancement in mice with EAE. (**A**) The typical disease course of EAE in SJL/J mice immunized with complete Freund's adjuvant and $PLP_{139-151}$. The red arrow corresponds to the imaging time point depicted in **B** and **C**. (**B**) EAE mice at 6 weeks post-immunization underwent MRI following intraperitoneal administration of gadolinium contrast. Note the presence of contrast enhancement involving the meninges (yellow arrows) either over the cortical surface (*left*) or deeper within the hippocampal fissure (*right*). This was noted both on MP-RAGE (*left*) and FLAIR (*right*) images. (**C**) We did not detect similar contrast enhancement in naïve SJL/J mice of a similar age. (**D**) In subsequent experiments we noted the presence of meningeal inflammation as early as 2 weeks post-immunization and there appeared to be an increase in the frequency and extent of meningeal enhancement over the course of the disease (from 2 weeks to >10 weeks post-immunization).

Leptomeningeal contrast-enhancing areas on MRI correspond to areas of meningeal inflammation

Following completion of imaging, mice were euthanized and tissues were obtained for histopathological evaluation. We noted the presence of dense cellular infiltrates in the subarachnoid space in the regions corresponding to meningeal contrast enhancement seen on MRI (Fig. 2A–D). We then performed immunohistochemistry to identify the cell populations comprising these meningeal infiltrates and found that the major components of the infiltrates were B220+ B lymphocytes (Figs 2E and 3A) and CD3+ T lymphocytes (Figs 2F and 3A). We also identified myeloid cells within these infiltrates expressing Mac2 (Fig. 3B) or IBA-1 (Fig. 3C), which are likely macrophages.

We also observed blood–meningeal barrier breakdown within these inflammatory infiltrates as evidenced by the presence of fibrinogen deposition (Fig. 3B). Interestingly, the pattern of fibrinogen deposition appeared to overlap with the distribution of Mac2+ myeloid cells (Fig. 3B). This is not surprising given the recent data regarding the ability of fibrinogen to signal to myeloid cells through the CD11b receptor.[28]

These results thus confirm previous reports of the presence of meningeal inflammation in SJL/J EAE and demonstrate the ability of contrast-enhanced MRI to detect areas of meningeal inflammation in SJL/J mice with EAE.

Areas of meningeal inflammation display markers of tertiary lymphoid tissue

Given previous reports that meningeal inflammation in a subset of patients with multiple sclerosis and mice with EAE demonstrates characteristics of tertiary lymphoid tissue, we stained for markers that would help identify this tissue type. We observed a network of FDC-M1+ follicular dendritic cells within the meningeal inflammatory infiltrates (Fig. 3D). We also stained for PNAd, a marker for high-endothelial venules normally found in lymphoid tissue, and identified the presence of PNAd+ vessel-like structures within a subset of the areas of meningeal inflammation (Fig. 3E). The presence of follicular dendritic cells and high-endothelial venules within areas of meningeal inflammation suggests that these areas may be organizing to form tertiary lymphoid structures.[29]

In addition, we noted the presence of cells staining for CXCL13 (Fig. 3F), a chemokine that is responsible for chemotaxis of B cells and which has been identified in ectopic lymphoid tissue.[19] Our results thus demonstrate the presence of features of tertiary lymphoid tissue in areas of meningeal inflammation in the SJL/J EAE model.

Meningeal inflammation is associated with pathological changes in adjacent cortex

Leptomeningeal inflammation has been linked to changes in the adjacent cortex, including cortical demyelination and neuronal dropout in patients with multiple sclerosis.[30,31] We first evaluated the effects on the cortex adjacent to areas of meningeal inflammation by examining changes in astrocytes and microglia. Using staining for GFAP we identified marked astrocytosis in the adjacent cortex (Fig. 4A and C) accompanied by a disruption of the glia limitans. In the same areas we also noted an increase in the number of IBA-1+ cells compared to controls (Fig. 4B and D). IBA-1+ cells in the cortex

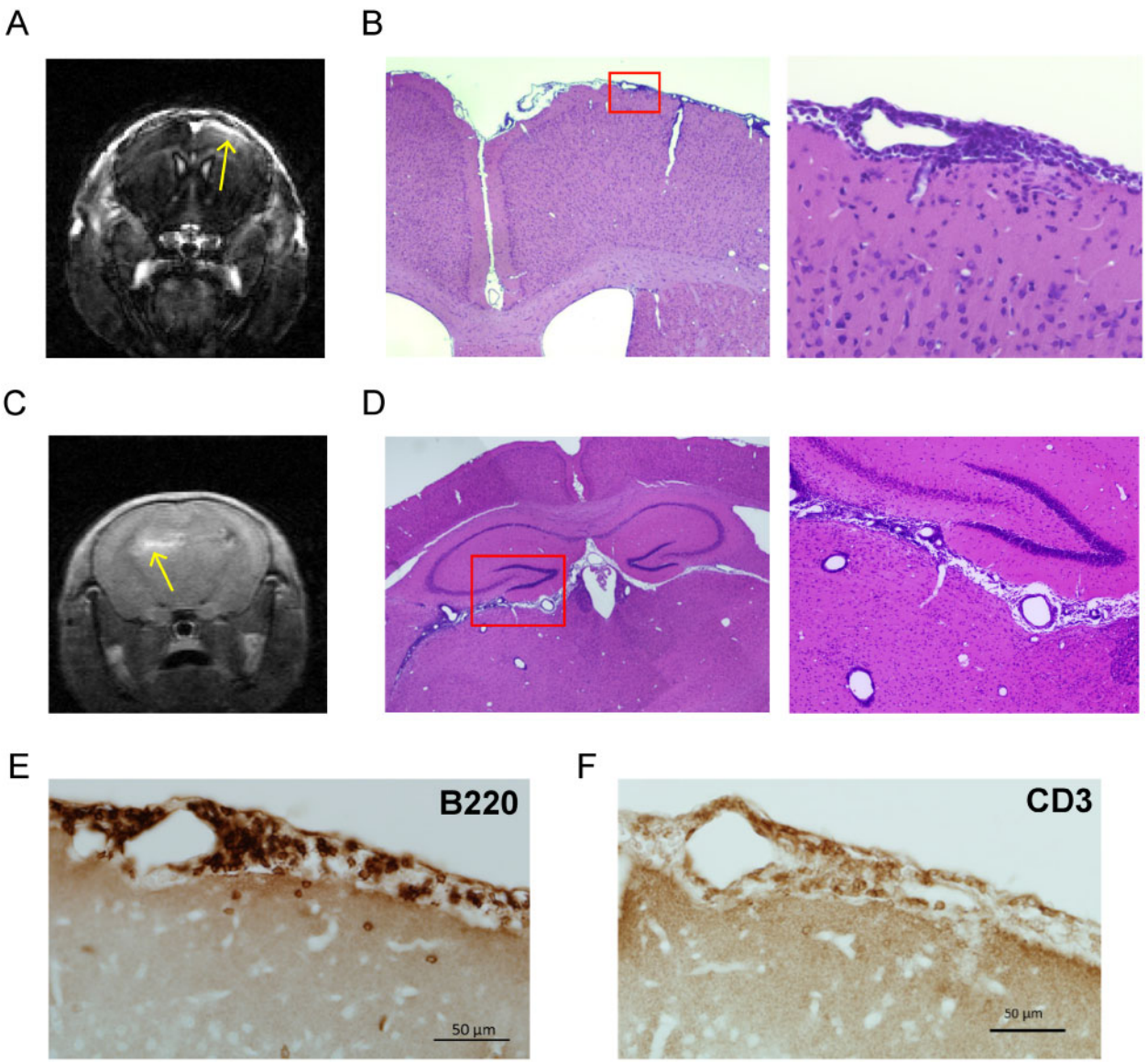

Figure 2 Areas of meningeal contrast enhancement correspond to leptomeningeal inflammation. (**A** and **C**) Following identification of areas of meningeal contrast enhancement on MRI we euthanized mice and obtained brain tissue for analysis. (**B** and **D**) On haematoxylin and eosin staining of the tissue corresponding to MRI areas of meningeal contrast enhancement we noted the presence of dense cellular infiltrates involving the leptomeninges. (**E**) In the areas of meningeal contrast enhancement, immunohistochemistry revealed the presence of numerous B220+ B cells and (**F**) CD3+ T cells.

adjacent to meningeal inflammation had an activated appearance as compared to those in the contralateral hemisphere that was unaffected by meningeal inflammation (Supplementary Fig. 2).

As recent data have demonstrated that cross-talk with microglia can determine the phenotype of astrocytes—and can lead to the development of reactive neurotoxic astrocytes[32,33]—we examined whether astrocytes in the cortex adjacent to areas of meningeal inflammation displayed markers of this phenotype (C3 and PSMB8). We detected C3+ and PSMB8+ GFAP+ cells (Supplementary Fig. 3) in the cortex adjacent to meningeal infiltrates, which may thus represent neurotoxic reactive astrocytes.

Since leptomeningeal inflammation in multiple sclerosis tissue is linked to greater cortical demyelination and neuronal damage, we evaluated myelin and axonal health in the cortex adjacent to meningeal infiltrates. We stained for myelin using Luxol fast blue dye and noted increased vacuolation and decreased staining in cortical areas adjacent to meningeal inflammation compared to controls (Fig. 5A).

To assess axonal stress/damage we performed staining for the non-phosphorylated form of neurofilament-H (SMI-32) and noted increased staining in the cortex adjacent to meningeal inflammation compared to control tissue (Fig. 5B and C). We obtained similar results using another marker of axonal stress and impaired fast axonal transport, namely amyloid precursor protein (APP),[34] and noted increased staining in the cortex adjacent to areas of meningeal inflammation compared to control tissue (Fig. 5D and E). This is consistent with impaired axonal transport of proteins that can occur with either axonal stress or damage.[35]

These results suggest a possible effect of meningeal inflammation on the underlying cerebral cortex with microglial and

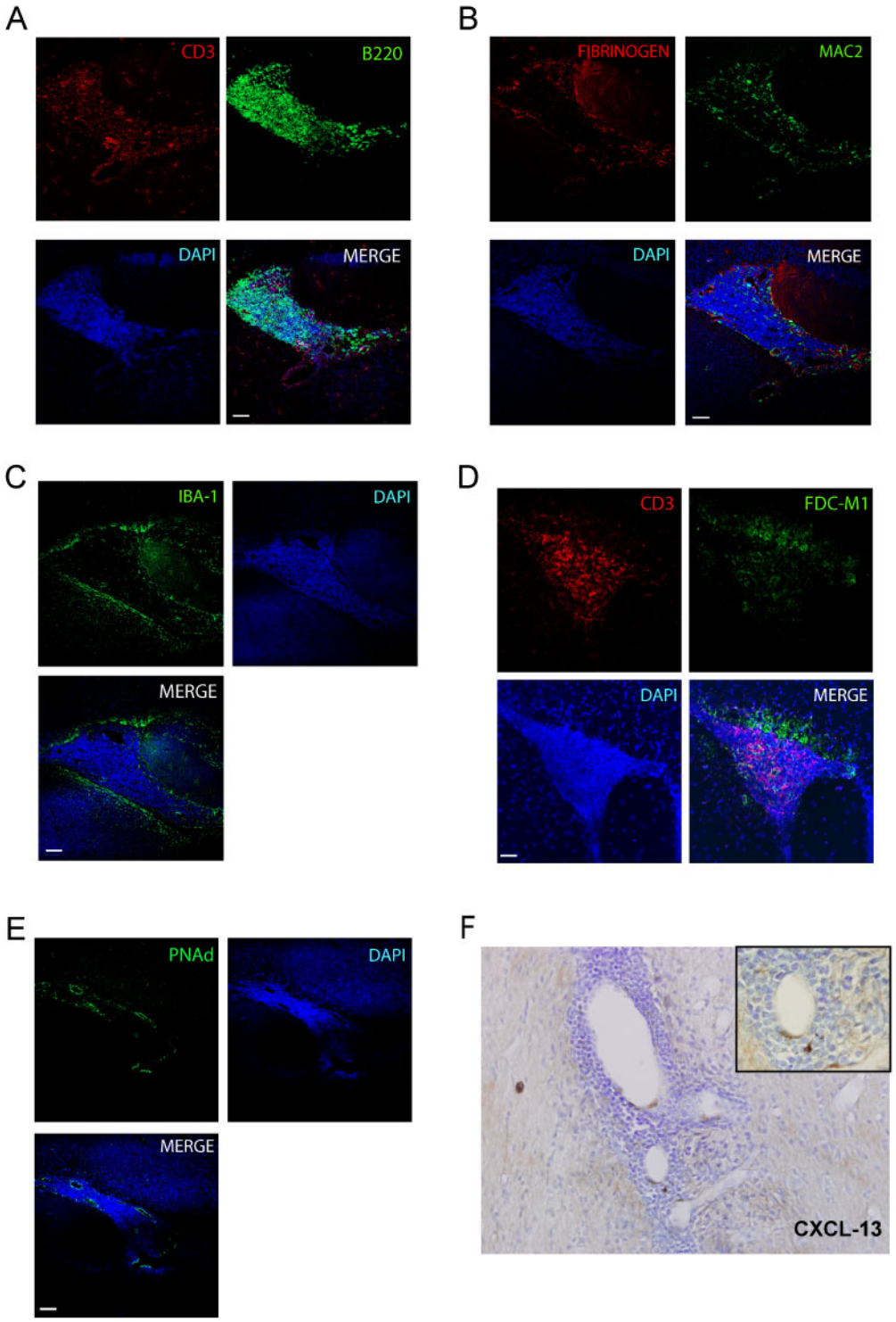

Figure 3 Leptomeningeal inflammatory infiltrates contain lymphocytes and myeloid cells and display markers of tertiary lymphoid tissue. (**A**) Areas of meningeal inflammation contained numerous CD3+ T cells and B220+ B cells. (**B**) These areas also demonstrated the presence of myeloid cells (Mac2+), and deposition of fibrinogen was noted consistent with breakdown of the blood–brain barrier resulting in contrast enhancement. Mac2+ cells appeared to cluster in areas of fibrinogen deposition. (**C**) IBA-1+ cells were observed, representing microglia and myeloid cells both within the areas of meningeal inflammation as well as the cortex surrounding these areas. (**D**) In addition, FDC-M1+ follicular dendritic cells were present within the leptomeningeal inflammatory infiltrates. (**E**) Other features consistent with tertiary lymphoid tissue included the presence of PNAd+ structures that were suggestive of high-endothelial venules and (**F**) CXCL13+ cells within these areas. Scale bars = 50 μm for all panels.

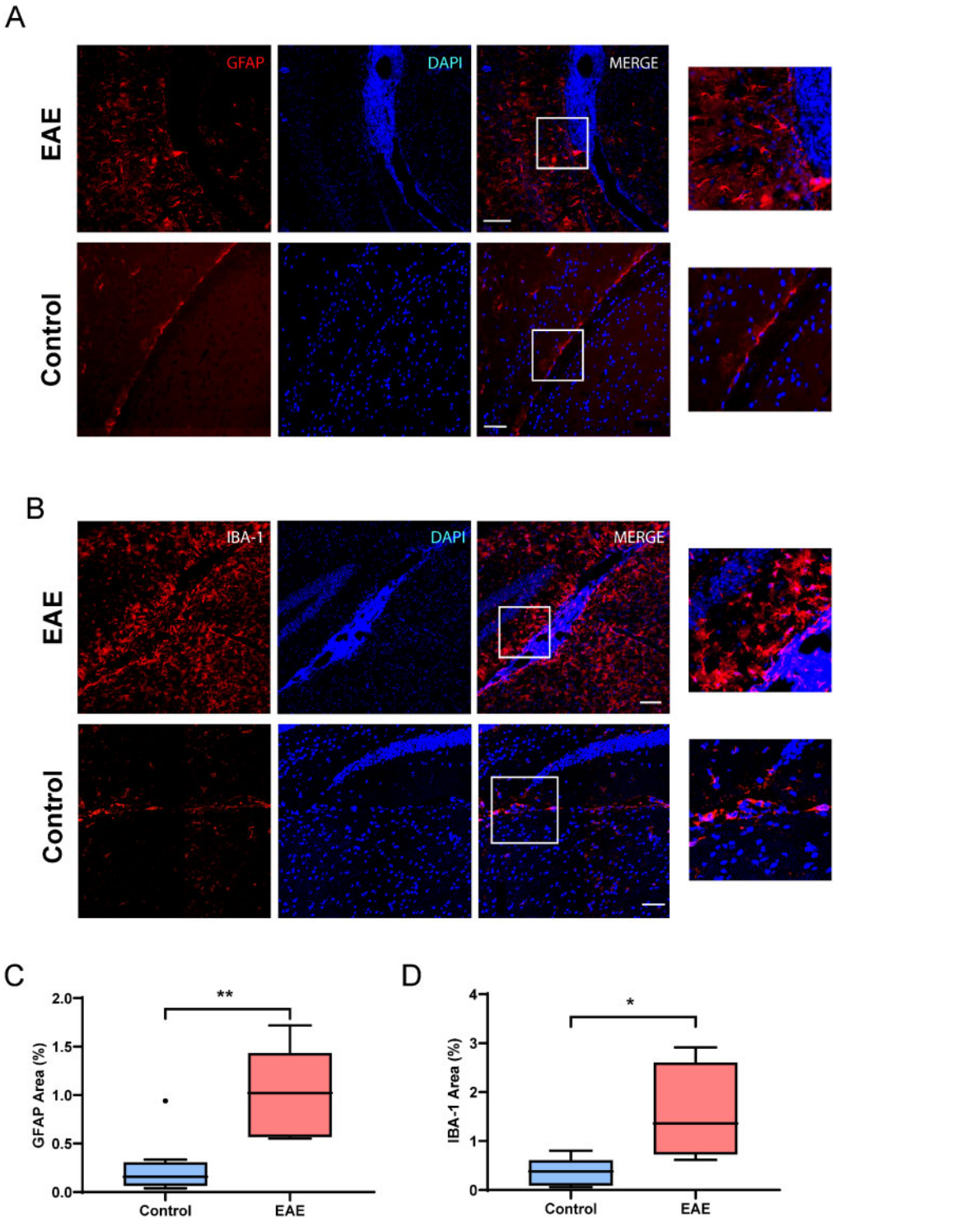

Figure 4 Cortex adjacent to leptomeningeal inflammation demonstrates astrocytosis and microgliosis. (**A**) Areas of the cortex adjacent to meningeal inflammation demonstrated increased numbers of astrocytes as well as disruption of the glia limitans as compared to control brain. This staining is quantified in **C**. (**B**) The cortex adjacent to areas of meningeal inflammation also demonstrated increased numbers of IBA-1+ cells and these cells appeared more activated compared to control brains. This staining is quantified in **D**. Scale bars = 100 μm in **A** and **B**. For **C** and **D** data are shown as box plots, the centre line indicates the median, the box indicates the 25th and 75th percentiles, the whiskers indicate 1.5 × interquartile range (IQR), and the dots indicate outliers. *P*-values are derived from a Mann-Whitney U-test. $^{**}P < 0.005$, $^{*}P < 0.05$.

astrocytic activation, demyelination and axonal damage. This is significant since these findings parallel the demyelination, axonal damage and neuronal damage noted in progressive multiple sclerosis patients with evidence of meningeal inflammation.

Longitudinal changes in meningeal enhancement and composition of meningeal infiltrates

Since imaging studies in multiple sclerosis have demonstrated the persistence of areas of leptomeningeal contrast enhancement over

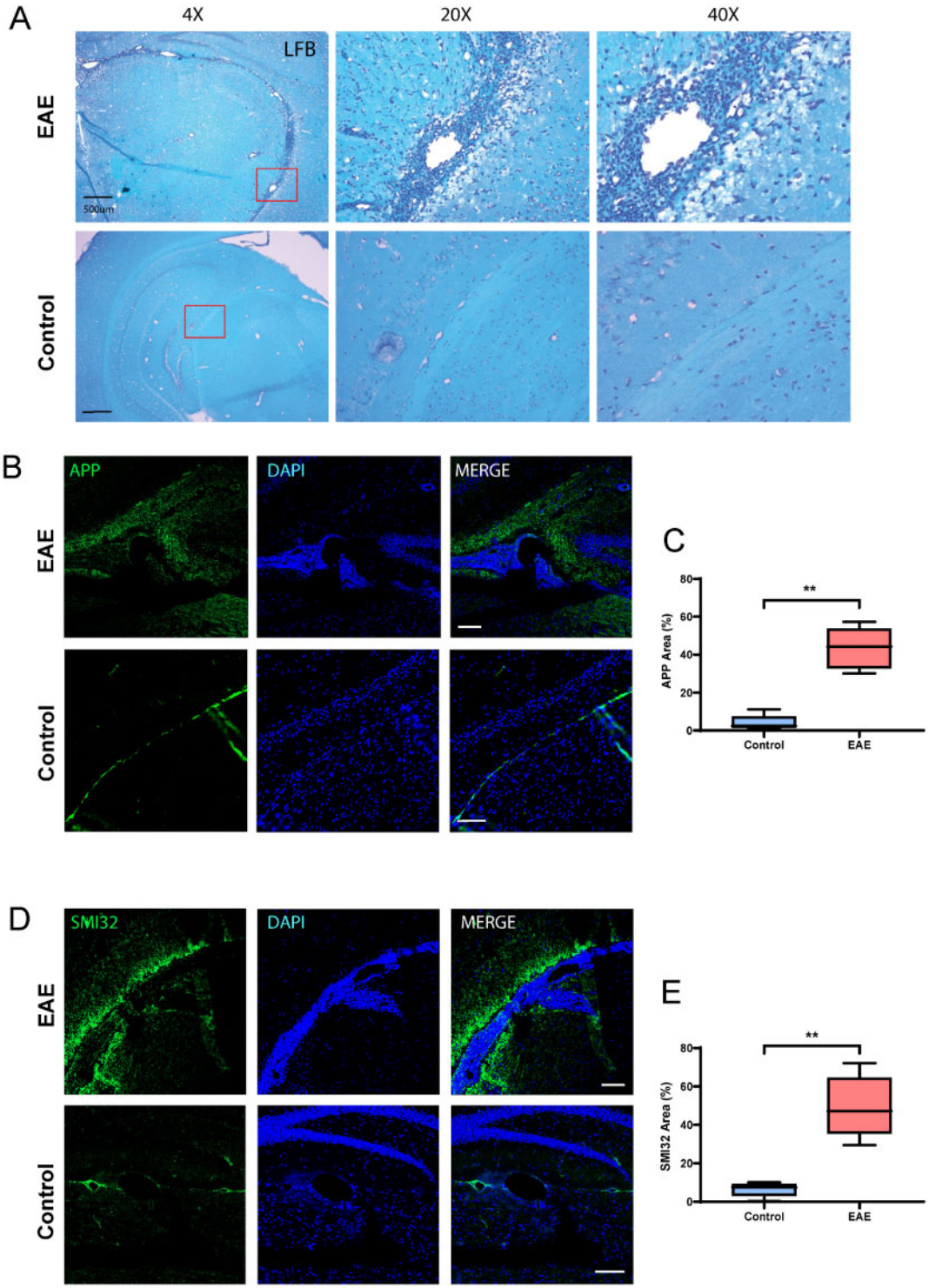

Figure 5 Cortex adjacent to leptomeningeal inflammation demonstrates axonal damage and demyelination. (**A**) We examined myelination using Luxol fast blue (LFB) staining in the cortex adjacent to areas of inflammation and noted increased demyelination (reduced staining and increased vacuolation) compared to normal brains. (**B**) We examined axonal stress/damage using staining for APP and noted increased staining in the cortex adjacent to meningeal inflammation compared to controls. (**C**) Quantification of APP staining in cortex adjacent to areas of meningeal inflammation in EAE compared to similar areas in controls. (**D**) We noted a similar increase in staining for non-phosphorylated neurofilament (SMI-32) in the cortex adjacent to areas of meningeal inflammation compared to control brains. (**E**) Quantification of SMI-32 staining in the cortex adjacent to areas of meningeal inflammation in EAE compared to similar areas in controls. Scale bars = 500 μm in **A**; 100 μm in **B** and **D**. Data in **C** and **E** are shown as box plots, the centre line indicates the median, the box indicates the 25th and 75th percentiles, the whiskers indicate 1.5 × IQR, and the dots indicate outliers. *P*-values are derived from a Mann-Whitney U-test. $^{**}P < 0.005$.

time, we performed longitudinal experiments to study the time course of these areas of meningeal inflammation. Mice were imaged serially at early (Week 2), middle (Week 4 or 6), and late (Week 8 or 10) time points. Lesions were identified at each time point, and tended to accumulate over time (Fig. 6A).

We also examined changes in the composition of meningeal infiltrates over time. In these experiments, mice that had evidence of meningeal contrast enhancement on MRI were sacrificed at early, middle or late time points and we performed immunostaining for T cells, B cells and myeloid cells. We noted a steady and

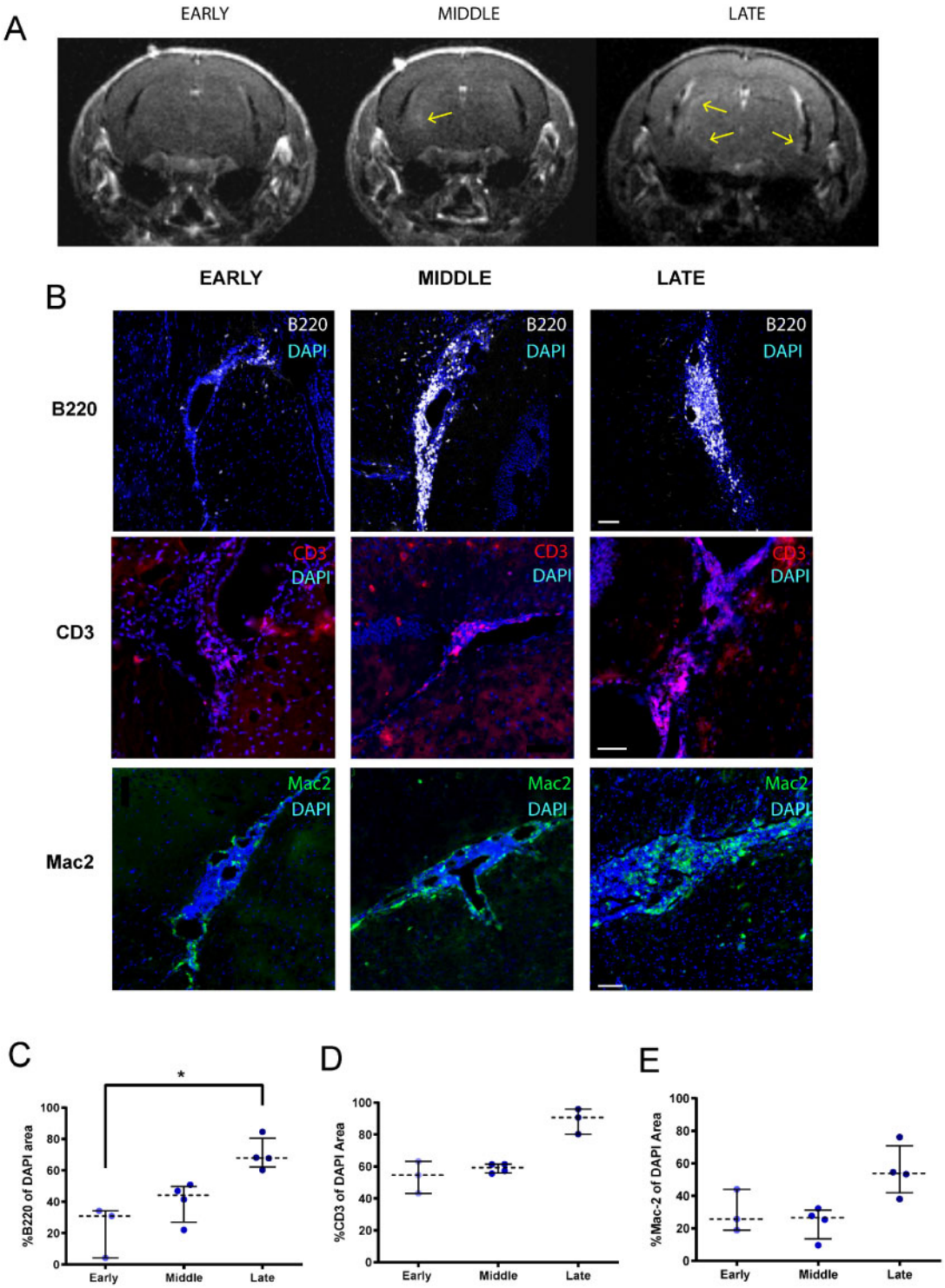

Figure 6 Leptomeningeal contrast enhancement persists over the course of EAE and the proportion of B cells increases in areas of leptomeningeal inflammation over time. (**A**) Leptomeningeal contrast enhancement persisted for several weeks and new areas accumulated over the course of EAE. (**B**) We also compared the composition of the meningeal inflammatory infiltrate over the course of EAE and noted changes in immune cell populations with a significant increase in the B-cell population within these areas (**C**). While the T cell (**D**) and myeloid cell (**E**) populations also appeared to increase over the course of EAE, these changes were not statistically significant. Scale bars = 50 μm in **B** (CD3); and 100 μm (B220 and Mac2). Data in **C–E** are shown as individual values and median ± IQR. *P*-values are derived from a Mann-Whitney U-test. *$P < 0.05$.

significant increase in the proportion of B cells in the inflammatory infiltrate over the course of EAE (Fig. 6B and C). This B-cell abundance is reminiscent of the leptomeningeal inflammation noted in multiple sclerosis patients.[6,36] While T cell and myeloid cell numbers also appeared to increase, this change was not statistically significant (Fig. 6B, D and E).

These results demonstrate that meningeal inflammation in rr-EAE can be detected by contrast-enhanced imaging and tends to persist over a period of several weeks, providing a potential marker for monitoring response to putative therapies. The composition of meningeal inflammation also evolves over time with a greater B cell abundance noted later in the course of rr-EAE.

BTK inhibition reduces meningeal inflammation and leptomeningeal contrast enhancement in mice

Since B cells are a major component of the meningeal infiltrate in multiple sclerosis patients, several trials have unsuccessfully attempted to target meningeal inflammation using anti-CD20 monoclonal antibodies.[16–18,38] Interestingly, in EAE mice treatment with an anti-CD20 antibody—which depletes peripheral B cells—did not result in a significant reduction in meningeal contrast enhancement compared to an isotype control antibody (Supplementary Fig. 4).

Given the presence of both B cell and myeloid populations in areas of meningeal inflammation, we tested whether an agent that targets both these cell populations would have an effect on leptomeningeal inflammation. Mice with evidence of meningeal contrast enhancement on MRI at 6 weeks post-immunization were randomized to either a BTK inhibitor—evobrutinib—or vehicle (Fig. 7A). We noted a significant reduction in meningeal contrast enhancement in the evobrutinib group but not in the vehicle group (Fig. 7B and C). There was also a small but significant effect on clinical score in the evobrutinib group compared to vehicle (Supplementary Fig. 5).

On pathological evaluation, a significant reduction was seen in the percentage of B cells within areas of meningeal inflammation (Fig. 7D and E). A similar trend was noted for T cells, but this was not statistically significant (Fig. 7D and F). However, myeloid cell infiltrates in the meninges appeared to persist despite B-cell depletion (Fig. 7D and G). We also noted a significant reduction in astrocytosis in the cortex surrounding areas of meningeal inflammation, suggesting that changes in the meningeal infiltrate were impacting inflammation in the adjacent cortex (Fig. 7D and H).

These results demonstrate that BTK inhibitor treatment reduced meningeal inflammation by altering the immune cell composition of meningeal inflammatory infiltrates and resulted in changes in the adjacent cortex.

Discussion

In this study we first demonstrated the ability of ultra-high field contrast-enhanced MRI to detect areas of meningeal contrast enhancement corresponding to meningeal inflammation in SJL/J mice with EAE. We then identified various pathological features of meningeal inflammation and their effects on the adjacent cortex that bear similarities to leptomeningeal inflammation in multiple sclerosis. Lastly, we demonstrated the utility of meningeal contrast enhancement as an outcome marker to assess the efficacy of treatment strategies targeting leptomeningeal inflammation. We observed a potential therapeutic role of a BTK inhibitor—evobrutinib—in ameliorating established meningeal inflammation in EAE, suggesting that this strategy warrants further investigation in humans.

While imaging of meningeal inflammation has been described in multiple sclerosis at 3 T and 7 T magnetic field strengths, only one other study has attempted to image this process in EAE.[39] In their study, Pol *et al.*[39] noted potential MRI changes representing meningeal inflammation which peaked at Day 10 post-immunization and then gradually declined over time. Unfortunately, the model chosen for that study does not develop persistent meningeal inflammation with significant B cell accumulation or the formation of tertiary lymphoid organs and hence it is unclear whether this approach would have produced results similar to those of our study had it been applied to the rr-EAE model.[19] We provide evidence that ultra-high field contrast-enhanced MRI can not only detect areas of meningeal inflammation, but also track this process over time. It could thus represent a potential surrogate marker of treatment response to help screen treatment modalities that impact meningeal inflammation.

We also characterized the meningeal infiltrate and obtained results similar to prior studies, demonstrating that areas of meningeal inflammation have an abundance of B and T lymphocytes. In addition, we noted the presence of myeloid cells including follicular dendritic cells. We also identified the presence of PNAd+ vessel-like structures consistent with high-endothelial venules. Thus, we noted some features consistent with tertiary lymphoid organ formation as previously described in both EAE and multiple sclerosis. The unique aspect of our study was that we evaluated changes in the meningeal infiltrate over an extended time period in EAE, and showed that the proportion of B cells within these areas continued to increase over the course of EAE: over 3-fold from Week 2 to Week 8–10 post-immunization. This is important when considering the timing of interventions that target this immune cell population.

In addition to examining the meningeal immune infiltrate, we also evaluated changes in the cortex adjacent to these areas. This is of interest because the major rationale for imaging and treating meningeal inflammation in multiple sclerosis is its potential relationship to increased cortical demyelination and neuronal loss. We identified the presence of increased axonal stress/damage, astrocytosis, microgliosis and demyelination in the cortex adjacent to areas of meningeal inflammation, similar to changes noted in multiple sclerosis. A recent study using an adoptive transfer approach in SJL mice also demonstrated similar changes in the cortex adjacent to areas of meningeal inflammation.[21] Future studies should also include behavioural testing to identify effects of meningeal inflammation on behaviour, learning and memory, and to determine whether the severity of meningeal inflammation is linked to the severity of these deficits, as EAE scores are primarily driven by spinal cord involvement.

The mechanism by which meningeal inflammation may contribute to the development of cortical changes is unknown. However, potential explanations include the production of antibodies or other soluble factors by B cells in the meninges, or the activation of macrophages/microglia or astrocytes in the cortex. We detected activated microglia/macrophages in the cortex and also observed C3+ and PSMB8+ astrocytes, which could indicate that there are reactive neurotoxic astrocytes in the cortex adjacent to areas of meningeal inflammation. Additional studies are required to identify the precise mechanism mediating cortical pathology in this model. Future studies could also examine the CSF to help identify the soluble factors that mediate cross-talk between meningeal inflammatory infiltrates and the adjacent cortex.

Since multiple clinical trials targeting meningeal inflammation in multiple sclerosis with B cell-depleting therapies have been unsuccessful, we decided to test an agent that targets both B lymphocytes and myeloid cells. BTK plays an important role in B cell development and in pro-inflammatory myeloid cell function.[24,25] We observed that over 4 weeks of treatment, evobrutinib reduced meningeal contrast enhancement compared to vehicle, and on

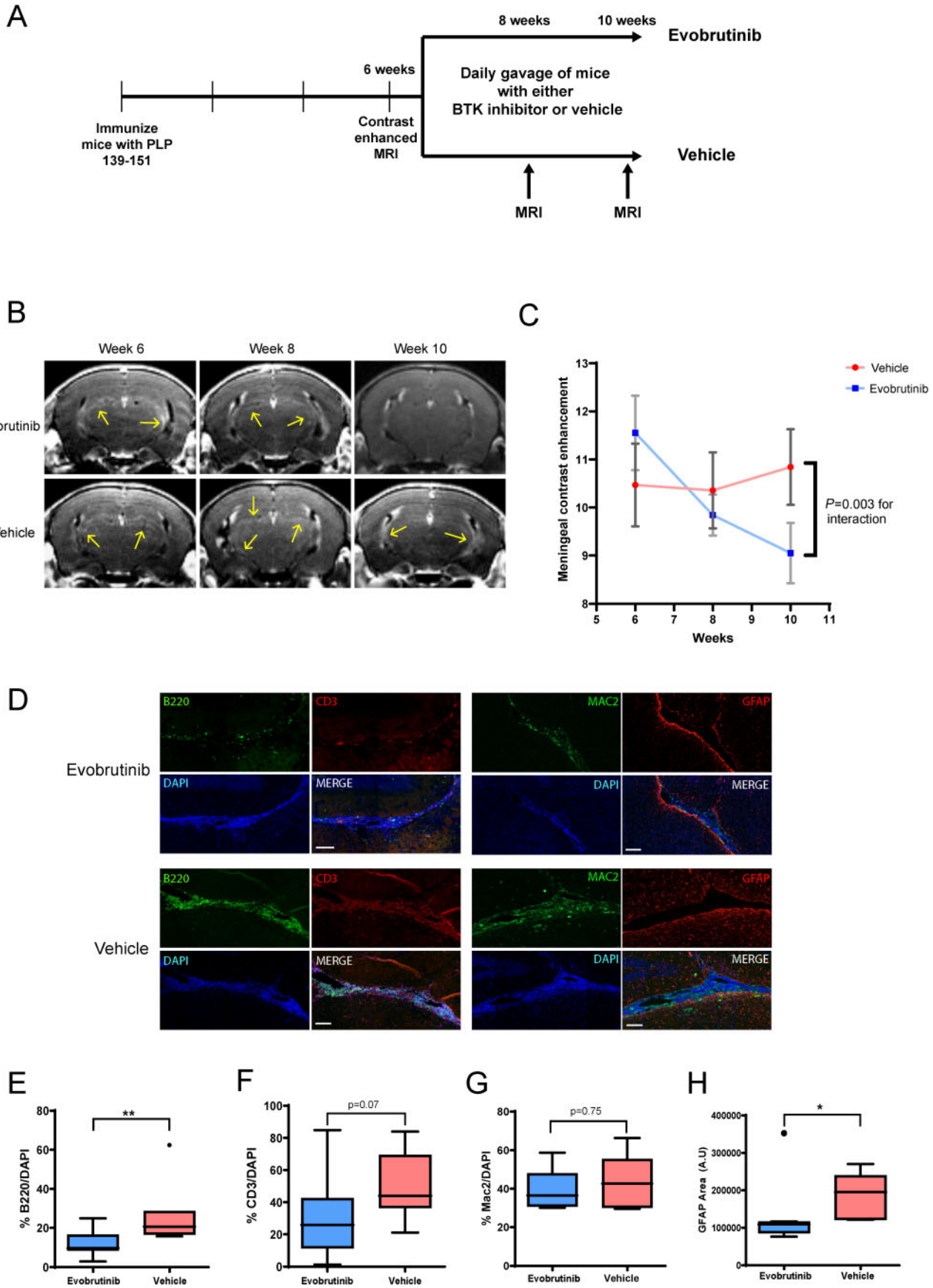

Figure 7 BTK inhibition reduced leptomeningeal inflammation detected on MRI and by histopathology. (**A**) Experimental design used to test the effect of a BTK inhibitor (evobrutinib) on established leptomeningeal inflammation in EAE. Mice with evidence of leptomeningeal contrast enhancement

(continued)

histopathology this corresponded to a decrease in B cells within the meningeal infiltrate. We also identified reduced astrocytosis in the adjacent cortex, suggesting that the effects on the meningeal infiltrate led to reduced pathology in the surrounding tissue. Evobrutinib has been shown to reduce relapse rate in patients with relapsing-remitting multiple sclerosis in a recent phase 2 trial with no significant serious adverse effects.[26] The results of the current study provide support for testing the effects of BTK inhibition in progressive multiple sclerosis and especially in patients with evidence of leptomeningeal inflammation.

In conclusion, we demonstrate the ability of ultra-high field contrast-enhanced MRI to detect and track meningeal inflammation in EAE and utilize this method to identify a novel potential therapeutic strategy to target meningeal inflammation in multiple sclerosis patients.

Acknowledgements

We thank Sanchaita Sonar for help with editing the manuscript. We thank Matthew Smith for technical assistance with this project.

Funding

This study was supported by a Career Transition Award (TA-1503-03465) from the National MS Society to P.B., a research grant from EMD-Serono to P.B., a John F Kurtzke Clinician Scientist Development Award from the American Academy of Neurology and grants from the Race to Erase MS to P.B. and P.A.C.

Competing interests

P.B. has received honoraria from EMD-Serono, Sanofi-Genzyme, MedDay Pharmaceuticals and GSK and research grants from EMD-Serono, Genentech and Amylyx Pharmaceuticals. S.K., A.A.R., P.V.Z., C.P., J.Z. and M.A. declare no competing interests. R.G. and U.B. are employees of EMD-Serono and Merck respectively. P.A.C. has received consulting fees from Disarm Therapeutics and Biogen and is PI on grants to JHU from Biogen and Annexon.

Supplementary material

Supplementary material is available at *Brain* online.

References

1. Jones JL, Phuah C-L, Cox AL, et al. IL-21 drives secondary autoimmunity in patients with multiple sclerosis, following therapeutic lymphocyte depletion with alemtuzumab (Campath-1H). *J Clin Invest*. 2009;119:2052-2061.
2. Serafini B, Rosicarelli B, Magliozzi R, et al. Detection of ectopic B-cell follicles with germinal centers in the meninges of patients with secondary progressive multiple sclerosis. *Brain Pathol*. 2004; 14:164-174.
3. Choi SR, Howell OW, Carassiti D, et al. Meningeal inflammation plays a role in the pathology of primary progressive multiple sclerosis. *Brain*. 2012;135:2925-2937.
4. Lucchinetti CF, Popescu BFG, Bunyan RF, et al. Inflammatory cortical demyelination in early multiple sclerosis. *N Engl J Med*. 2011;365:2188-2197.
5. Absinta M, Vuolo L, Rao A, et al. Gadolinium-based MRI characterization of leptomeningeal inflammation in multiple sclerosis. *Neurology*. 2015;85:18-28.
6. Magliozzi R, Howell O, Vora A, et al. Meningeal B-cell follicles in secondary progressive multiple sclerosis associate with early onset of disease and severe cortical pathology. *Brain*. 2007;130: 1089-1104.
7. Howell OW, Reeves C. A, Nicholas R, et al. Meningeal inflammation is widespread and linked to cortical pathology in multiple sclerosis. *Brain*. 2011;134:2755-2771.
8. Harrison DM, Wang KY, Fiol J, et al. Leptomeningeal enhancement at 7T in multiple sclerosis: Frequency, morphology, and relationship to cortical volume. *J Neuroimaging*. 2017;27:461-468.
9. Zurawski J, Tauhid S, Chu R, et al. 7T MRI cerebral leptomeningeal enhancement is common in relapsing-remitting multiple sclerosis and is associated with cortical and thalamic lesions. *Mult Scler J*. 2020;26:177-187.
10. Absinta M, Cortese ICM, Vuolo L, et al. Leptomeningeal gadolinium enhancement across the spectrum of chronic neuroinflammatory diseases. *Neurology*. 2017;88:1439-1444.
11. Absinta M, Ontaneda D. Controversial association between leptomeningeal enhancement and demyelinated cortical lesions in multiple sclerosis. *Mult Scler J*. 2020;26:135-136.
12. Bergsland N, Ramasamy D, Tavazzi E, et al. Leptomeningeal contrast enhancement is related to focal cortical thinning in relapsing-remitting multiple sclerosis: A cross-sectional MRI study. *AJNR Am J Neuroradiol*. 2019;40:620-625.
13. Makshakov G, Magonov E, Totolyan N, et al. Leptomeningeal contrast enhancement is associated with disability progression and grey matter atrophy in multiple sclerosis. *Neurol Res Int*. 2017;2017:1-7.
14. Zivadinov R, Ramasamy DP, Vaneckova M, et al. Leptomeningeal contrast enhancement is associated with progression of cortical atrophy in MS: A retrospective, pilot, observational longitudinal study. *Mult Scler J*. 2017;23:1336-1345.
15. Bergman J, Burman J, Gilthorpe JD, et al. Intrathecal treatment trial of rituximab in progressive MS. *Neurology*. 2018;91:e1893-e1901.
16. Bhargava P, Wicken C, Smith MD, et al. Trial of intrathecal rituximab in progressive multiple sclerosis patients with evidence of leptomeningeal contrast enhancement. *Mult Scler Relat Disord*. 2019;30:136-140.
17. Komori M, Lin YC, Cortese I, et al. Insufficient disease inhibition by intrathecal rituximab in progressive multiple sclerosis. *Ann Clin Transl Neurol*. 2016;3:166-179.
18. Topping J, Dobson R, Lapin S, et al. The effects of intrathecal rituximab on biomarkers in multiple sclerosis. *Mult Scler Relat Disord*. 2016;6:49-53.
19. Magliozzi R, Columba-Cabezas S, Serafini B, et al. Intracerebral expression of CXCL13 and BAFF is accompanied by formation of

Figure 7 Continued
were randomized to either vehicle or evobrutinib and treated for 4 weeks. (**B**) We noted a reduction in contrast enhancement with evobrutinib treatment as compared to vehicle over the 4-week treatment period. This is quantified in **C**. (**D** and **E**) On pathological evaluation at Week 10, we noted a reduction in the proportion of B cells within the meningeal infiltrate in the evobrutinib group compared to vehicle. A similar trend was noted for T cells but was not significant (**D** and **F**). There was no significant difference in the proportion of myeloid cells (Mac2 +) (**D** and **G**). (**D** and **H**) We noted a reduction in GFAP+ cells in the cortex adjacent to the areas of meningeal inflammation in the evobrutinib group compared to vehicle. For **E** and **F**, $n = 11$ for the evobrutinib group and $n = 7$ for the vehicle group; for **G** and **H**, $n = 8$ for the evobrutinib group and $n = 6$ for the vehicle group. Scale bars = 100 μm in **D**. For **E**–**H**, data are shown as box plots, the centre line indicates the median, the box indicates the 25th and 75th percentiles, the whiskers indicate 1.5 × IQR, and the dots indicate outliers. *P*-values are derived from a Mann-Whitney U-test. $^{*}P < 0.05$, $^{**}P < 0.005$.

lymphoid follicle-like structures in the meninges of mice with relapsing experimental autoimmune encephalomyelitis. *J Neuroimmunol*. 2004;148:11-23.
20. Pikor NB, Astarita JL, Summers-Deluca L, et al. Integration of Th17- and lymphotoxin-derived signals initiates meningeal-resident stromal cell remodeling to propagate neuroinflammation. *Immunity*. 2015;43:1160-1173.
21. Ward LA, Lee DS, Sharma A, et al. Siponimod therapy implicates Th17 cells in a preclinical model of subpial cortical injury. *JCI Insight*. 2020;5:e132522.
22. Christy AL, Walker ME, Hessner MJ, et al. Mast cell activation and neutrophil recruitment promotes early and robust inflammation in the meninges in EAE. *J Autoimmun*. 2013;42:50-61.
23. Parker Harp CR, Archambault AS, Cheung M, et al. Neutrophils promote VLA-4–dependent B cell antigen presentation and accumulation within the meninges during neuroinflammation. *Proc Natl Acad Sci USA*. 2019;116:24221-24230.
24. Gabhann JN, Hams E, Smith S, et al. Btk regulates macrophage polarization in response to lipopolysaccharide. *PLoS One*. 2014;9:e85834.
25. Haselmayer P, Camps M, Liu-Bujalski L, et al. Efficacy and pharmacodynamic modeling of the BTK inhibitor evobrutinib in autoimmune disease models. *J Immunol*. 2019;202:2888-2906.
26. Montalban X, Arnold DL, Weber MS, et al. Placebo-controlled trial of an oral BTK inhibitor in multiple sclerosis. *N Engl J Med*. 2019;380:2406-2417.
27. Tsuchiya K, Katase S, Yoshino A, et al. FLAIR MR imaging for diagnosing intracranial meningeal carcinomatosis. *Am J Roentgenol*. 2001;176:1585-1588.
28. Ryu JK, Petersen MA, Murray SG, et al. Blood coagulation protein fibrinogen promotes autoimmunity and demyelination via chemokine release and antigen presentation. *Nat Commun*. 2015;6:8164.
29. Luo S, Zhu R, Yu T, et al. Chronic inflammation: A common promoter in tertiary lymphoid organ neogenesis. *Front Immunol*. 2019;10:2938.
30. Howell OW, Schulz-Trieglaff EK, Carassiti D, et al. Extensive grey matter pathology in the cerebellum in multiple sclerosis is linked to inflammation in the subarachnoid space. *Neuropathol Appl Neurobiol*. 2015;41:798-813.
31. Magliozzi R, Howell OW, Reeves C, et al. A gradient of neuronal loss and meningeal inflammation in multiple sclerosis. *Ann Neurol*. 2010;68:477-493.
32. Liddelow SA, Guttenplan KA, Clarke LE, et al. Neurotoxic reactive astrocytes are induced by activated microglia. *Nature*. 2017;541:481-487.
33. Rothhammer V, Borucki DM, Tjon EC, et al. Microglial control of astrocytes in response to microbial metabolites. *Nature*. 2018;557:724-728.
34. Medana IM, Esiri MM. Axonal damage: A key predictor of outcome in human CNS diseases. *Brain*. 2003;126:515-530.
35. Schirmer L, Antel JP, Brück W, et al. Axonal loss and neurofilament phosphorylation changes accompany lesion development and clinical progression in multiple sclerosis. *Brain Pathol*. 2011;21:428-440.
36. Wicken C, Nguyen J, Karna R, et al. Leptomeningeal inflammation in multiple sclerosis: Insights from animal and human studies. *Mult Scler Relat Disord*. 2018;26:173-182.
37. Svenningsson A, Bergman J, Dring A, et al. Rapid depletion of B lymphocytes by ultra-low-dose rituximab delivered intrathecally. *Neurol Neuroimmunol Neuroinflamm*. 2015;2:e79.
38. Pol S, Schweser F, Bertolino N, et al. Characterization of leptomeningeal inflammation in rodent experimental autoimmune encephalomyelitis (EAE) model of multiple sclerosis. *Exp Neurol*. 2019;314:82-90.